

# Distribution Embedding Networks for Meta-Learning with Heterogeneous Covariate Spaces

Lang Liu<sup>1</sup>      Mahdi Milani Fard<sup>2</sup>      Sen Zhao<sup>2</sup>

<sup>1</sup> Department of Statistics, University of Washington

<sup>2</sup> Google Research

## Abstract

We propose Distribution Embedding Networks (DEN) for classification with small data using meta-learning techniques. Unlike existing meta-learning approaches that focus on image recognition tasks and require the training and target tasks to be similar, DEN is specifically designed to be trained on a diverse set of training tasks and applied on tasks whose number and distribution of covariates differ vastly from its training tasks. Such property of DEN is enabled by its three-block architecture: a covariate transformation block followed by a distribution embedding block and then a classification block. We provide theoretical insights to show that this architecture allows the embedding and classification blocks to be fixed after pre-training on a diverse set of tasks; only the covariate transformation block with relatively few parameters needs to be updated for each new task. To facilitate the training of DEN, we also propose an approach to synthesize binary classification training tasks, and demonstrate that DEN outperforms existing methods in a number of synthetic and real tasks in numerical studies.

## 1 Introduction

While deep learning has made substantial progress in supervised learning, its success usually relies on a large number of labeled examples. However, in many real-world applications, it is costly to collect large training sets. For example, in online abuse detection, at any time, we may only possess dozens of freshly labeled abuse results. In health sciences, we may only have clinical outcomes on a few study subjects. Meta-learning aims to tackle the small data problem by training a model on labeled data from a number of related tasks, with the goal to perform well on similar, but unseen future tasks with a small amount of labeled observations.

Existing meta-learning techniques often assume a homogeneous feature space across tasks. For instance, in image classification, the features are all pixels and we can usually crop images to get the same number of features. However, in many other tasks with tabular data, such as the ones mentioned above, it is common that there are not sufficient labeled data in the covariate space of the target task, while labeled data in other covariate spaces are abundant. Existing methods cannot be applied in such cases with heterogeneous covariate spaces across tasks, i.e., their covariates live in different spaces, having different distributions with possibly different dimensions. Although learning from heterogeneous feature spaces has been studied in transfer learning Dai et al. (2008); Yang et al. (2009); Wang and Mahadevan (2011); Zhou et al. (2014); Li et al. (2014); Yan et al. (2017); Zhou et al. (2019), these approaches only focus on two tasks (source and target), and the strategy is to learn a transformation mapping to project the source task and the target task into the same space. In contrast, Iwata and Kumagai (2020) consider meta-learning with heterogeneous attribute spaces, but their approach is more restrictive compared to the method proposed in this work; see Section 2.

In this work, we propose Distribution Embedding Networks (DEN) for meta-learning with heterogeneous covariate spaces. In the same spirit of feature transformation in transfer learning literature, we first calibrate the raw covariates (*task-dependent* transformation block). An embedding of the transformed covariates is averaged over the target-task training data to form a “task summary” embedding vector (*task-independent*

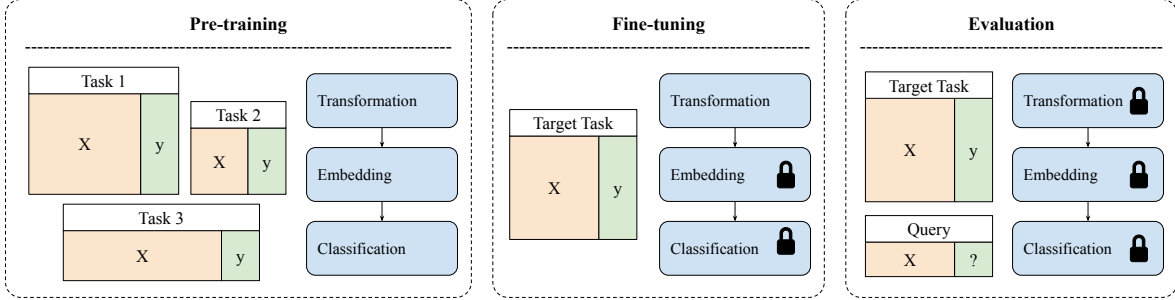


Figure 1: Training and evaluation of DEN. We first pre-train DEN on training tasks with heterogeneous covariate spaces. We then fine-tune the transformation block on a labeled sample from the target task, and use the fine-tuned model for classification on the query set.

distribution embedding block). This task summary is then used in the final classifier applied to query examples (*task-independent* classification block).

As illustrated in Figure 1, this three-block architecture allows us to *pre-train* the model on a large collection of tasks with heterogeneous covariate spaces, and use a few examples from the target task to *fine-tune* the task-dependent transformation block with only a small number of parameters. The embedding and classification blocks will be kept fixed after pre-training. Pre-training can even be done on synthesized classification tasks, as we illustrate in Section 5.

To summarize our main contributions: (I) We propose a method for meta-learning with heterogeneous covariate spaces – an important setting that expands the applications of meta-learning but has rarely been investigated in the literature; (II) The proposed model has a novel three-block architecture, allowing it to be pre-trained on a large variety of tasks, and then fine-tuned on an unrelated target task; (III) We provide theoretical insights on the three-block architecture of DEN; (IV) We design a procedure to generate artificial tasks for pre-training, and empirically verify its effectiveness when testing on real tasks; (V) We compare DEN with various existing meta-learning approaches on both simulated and real tasks, showing improved performance in most of the tasks we consider.

## 2 Related Work

There are multiple generic techniques applied to the meta-learning problem in the literature (Wang et al., 2020). The first camp learns similarities between pairs of examples using embeddings (Koch et al., 2015; Vinyals et al., 2016; Bertinetto et al., 2016; Snell et al., 2017; Oreshkin et al., 2018; Wang et al., 2018; Sung et al., 2018; Satorras and Estrach, 2018; Liu et al., 2019; Mishra et al., 2018). The second camp of optimization-based meta-learning aims to find a good starting point model such as different variants of MAML (Finn et al., 2017; Lee and Choi, 2018; Finn et al., 2018; Grant et al., 2018; Rusu et al., 2019) and Meta-Learner LSTM (Ravi and Larochelle, 2017). The third camp utilizes memory (Santoro et al., 2016; Kaiser et al., 2017; Munkhdalai and Yu, 2017; Munkhdalai et al., 2018). The fourth camp is conceptually similar to topic modeling, such as Neural Statistician (Edwards and Storkey, 2017) and CNP (Garnelo et al., 2018). However, these methods assume that all training and target tasks share the same feature spaces.

Learning from heterogeneous feature spaces has been studied in transfer learning, or domain adaptation Dai et al. (2008); Yang et al. (2009); Wang and Mahadevan (2011); Duan et al. (2012); Zhou et al. (2014); Li et al. (2014); Yan et al. (2017); Zhou et al. (2019); see Day and Khoshgoftaar (2017) for a survey. These approaches focus on two tasks (source and target), and require us to learn a transformation mapping to project the source and target tasks into the same space.

In contrast, Iwata and Kumagai (2020) consider meta-learning with heterogeneous attribute spaces. Both their approach and DEN rely on pooling to handle variable length inputs, using building blocks such as Deep Sets Zaheer et al. (2017) and Set Transformers Lee et al. (2019). There are several differences between their

approach and DEN. Firstly, DEN uses a covariate transformation block, relaxing the requirement that the covariates in training and target tasks come from the same distribution family. This further expands the scope of applications since collecting related training tasks can be challenging in some situations. Secondly, their model is permutation invariant in covariates and thus restrictive in model expressiveness; while DEN does not have this restriction. Thirdly, we also provide further theoretical insights and justification for the our model architecture design.

### 3 Notations

Let  $\mathbb{T}_1, \dots, \mathbb{T}_M$  be training tasks. For each training task  $\mathbb{T}$ , we observe an i.i.d. sample  $\mathcal{D}_{\mathbb{T}} = \{(\mathbf{x}_{\mathbb{T},i}, y_{\mathbb{T},i})\}_{i \in [n_{\mathbb{T}}]}$  from some joint distribution  $P_{\mathbb{T}}$ , where  $[n] = \{1, \dots, n\}$  and  $\mathbf{x}_{\mathbb{T},i} \in \mathbb{R}^{d_{\mathbb{T}}}$  is the covariates of the  $i$ -th example and  $y_{\mathbb{T},i} \in [L_{\mathbb{T}}]$  is its associated label. We denote this sample in matrix form by  $(\mathbf{X}_{\mathbb{T}}, \mathbf{y}_{\mathbb{T}})$ , where the  $j$ -th column  $\mathbf{x}_{\mathbb{T}}^j \in \mathbb{R}^{n_{\mathbb{T}}}$  is the  $j$ -th covariate vector. We let  $\mathbf{X}_{\mathbb{T},k}$  be the covariate sub-matrix corresponding to examples with label  $k$  for  $k \in [L_{\mathbb{T}}]$ . When the context is clear, we drop the dependency on  $\mathbb{T}$  for simplicity of the notation, e.g., we write  $\mathbf{X}_{\mathbb{T},k}$  as  $\mathbf{X}_k$ .

Let  $\mathbb{S}$  be a target task that is not contained in the training tasks. We are given a set of labeled examples  $(\mathbf{X}_{\mathbb{S}}, \mathbf{y}_{\mathbb{S}})$ , where the sample size  $n_{\mathbb{S}}$  is small. We refer to it as the *support set*. The goal is to predict labels for unlabeled examples in the target task, which is called the *query set*. We denote  $\mathcal{T} = \{\mathbb{T}_1, \dots, \mathbb{T}_M, \mathbb{S}\}$ .

## 4 Distribution Embedding Networks

### 4.1 Model Architecture for Binary Classification

To describe the model architecture of DEN for binary classification (illustrated in Figure 2), consider data  $(\mathbf{X}, \mathbf{y})$  in a given task  $\mathbb{T}$ .

**Transforming raw inputs with task-dependent covariate transformation block.** We first transform the raw inputs via a covariate transformation block, i.e.,

$$\mathbf{Z} = c(\mathbf{X}), \quad (1)$$

where  $c : \mathbb{R}^d \rightarrow \mathbb{R}^d$  is applied to each row. Specifically, we use a piecewise linear function<sup>1</sup> (PLF) for each covariate, i.e.,  $c(\mathbf{x}) = (c^1(x^1), \dots, c^d(x^d))$ . We can optionally constrain the PLFs to be monotonic, which would serve as a form of regularization during training (Gupta et al., 2016). Note that the transformation block is the only task-dependent block for DEN, whose parameters need to be retrained for each new task.

One may instead consider other transformation blocks. We choose PLFs since they can implement compact one-dimensional non-linearities and can thus be fine-tuned with a small support set. Moreover, they are universal approximators in this space: with enough keypoints, they can approximate any bounded continuous functions. In Section 5 we show that this PLF transformation is key to ensure good performance when training tasks and target tasks have heterogeneous covariate spaces; we also study the tradeoffs between the flexibility of PLF and the size of the support set.

**Summarizing task statistics with task-independent distribution embedding block.** We embed the distribution  $P(\mathbf{z}, y)$  into a vector using the transformed features  $\mathbf{Z}$  of the support set in the following way. For all  $a, b \in [d]$ , we derive a distribution embedding of  $P(z^a, z^b, y)$  by

$$\mathbf{s}^{a,b} = \left( \frac{1}{n_1} \sum_{i=1}^n h(z_i^a, z_i^b) \mathbf{1}\{y_i = 1\}, \frac{1}{n_2} \sum_{i=1}^n h(z_i^a, z_i^b) \mathbf{1}\{y_i = 2\}, \frac{1}{n} \sum_{i=1}^n y_i \right), \quad (2)$$

---

<sup>1</sup>See Appendix A for the precise definition.

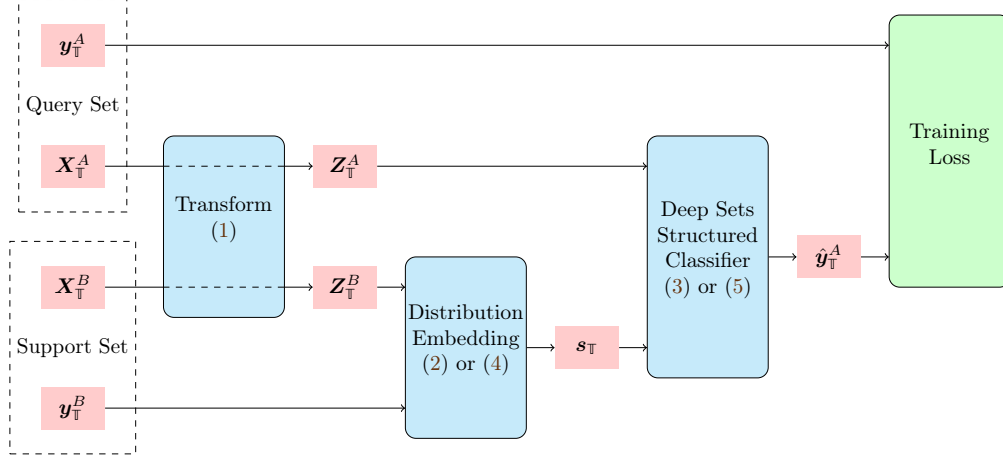


Figure 2: Block diagram of the DEN model for binary classification. During pre-training, for each gradient step we sample task  $\mathbb{T}$ , query set  $(\mathbf{X}_{\mathbb{T}}^A, \mathbf{y}_{\mathbb{T}}^A)$  and support set  $(\mathbf{X}_{\mathbb{T}}^B, \mathbf{y}_{\mathbb{T}}^B)$ . We fine-tune the task-dependent transformation block on the target task  $\mathbb{S}$  to get  $c_{\mathbb{S}}$ .

Table 1: Overview of training and evaluation.

Step	Input data	Transformation	Embedding	Classification
Pre-training	Data from a set of tasks $\{(\mathbf{x}_{\mathbb{T},i}, \mathbf{y}_{\mathbb{T},i})\}_{\mathbb{T},i}$	Trained	Trained	Trained
Fine-tuning	Support set from the target task $\{(\mathbf{x}_{\mathbb{S},i}, \mathbf{y}_{\mathbb{S},i})\}_i$	Trained $c_{\mathbb{S}}$	Fixed	Fixed
Evaluation	Query input $\mathbf{x}_{\mathbb{S},q}$ and support set $\{(\mathbf{x}_{\mathbb{S},i}, \mathbf{y}_{\mathbb{S},i})\}_i$	Fixed $c_{\mathbb{S}}$	Fixed	Fixed

where  $h$  is a vector-valued *trainable* function and  $n_k = \sum_{i=1}^n \mathbf{1}\{y_i = k\}$  for  $k \in \{1, 2\}$ . Note that the same function  $h$  is shared across all tasks, and it can be chosen as fully connected layers. The distribution  $P(\mathbf{z}, y)$  is then embedded as the concatenation  $\mathbf{s} = (\mathbf{s}^{a,b})_{a,b \in [d]}$ . Intuitively, we decompose a variable-length feature vector  $\mathbf{z}$  into smaller pieces of fixed length 2, and obtain a distribution embedding for each of the pieces. This, together with the following classification block, allows us to handle variable-length inputs.

*Remark 4.1.* The length 2 here is not essential. We can use pieces of length  $r$  for any  $r \geq 1$ , i.e., obtain an embedding  $\mathbf{s}^{t_1, \dots, t_r}$  of  $P(\mathbf{z}^{t_1, \dots, t_r}, y)$  for all  $t_1, \dots, t_r \in [d]$ . The larger  $r$  is the more expressive but more expensive the model will be. We refer to  $r$  as the *dependency order*. We will experiment with different values of  $r$  in Section 5.

**Prediction with task-independent classification block.** Given a query  $\mathbf{x}$ , we first transform it via  $\mathbf{z} = c(\mathbf{x})$  and concatenate it with the distribution embedding  $\mathbf{s}^{a,b}$  in (2). We then obtain the predicted probability using a Deep Sets architecture [Zaheer et al. \(2017\)](#):

$$q = \Phi(\mathbf{z}, \mathbf{s}) = \psi \left( \sum_{a,b \in [d]} \varphi(\mathbf{z}^{a,b}, \mathbf{s}^{a,b}) \right), \quad (3)$$

where  $\varphi$  is a vector-valued trainable function and  $\psi$  is a real-valued trainable function. Both of them are shared across tasks and can be chosen as fully connected layers. We note that one may use other structures to construct the classification block, e.g., Set Transformer [Lee et al. \(2019\)](#).

## 4.2 Model Architecture for Multiclass Classification

For multiclass classification tasks, we modify the distribution embedding in (2) as

$$\mathbf{s}^{a,b} = \frac{1}{n} \sum_{i=1}^n h(z_i^a, z_i^b, \mathbf{v}(y_i)), \quad (4)$$

where  $\mathbf{v}(k)$  is a vector encoding of the class  $k$ , e.g., one-hot encoding. Note that we allow the number of classes to vary across tasks, while the encoding  $\mathbf{v}$  is shared across tasks.

For the classification block, we modify the idea of Matching Net (Vinyals et al., 2016), which is also similar to the modification adopted by Iwata and Kumagai (2020). This modification is suitable for tasks with different numbers of label classes. Let  $\tilde{\Phi}$  be  $\Phi$  without the last layer. For each query set example with PLF-transformed feature  $\mathbf{z}$ , we obtain its class scores by

$$q_k = \frac{\sum_{i=1}^n \tilde{\Phi}(\mathbf{z}, \mathbf{s})^\top \tilde{\Phi}(\mathbf{z}_i, \mathbf{s}) \mathbf{1}\{y_i = k\}}{\sum_{i=1}^n \mathbf{1}\{y_i = k\}}, \quad (5)$$

and then use a softmax layer to get class probabilities. Note that  $i$  in the above equation is the index of support set examples ( $n$  in total), and  $\tilde{\Phi}(\mathbf{z}, \mathbf{s})$  is a column vector of the embedding before the final classification.

## 4.3 Justification for the Architecture Design

For further insights into the model architecture, consider the optimal Bayes classifier:

$$P(y = k | \mathbf{x}) = \frac{P(\mathbf{x} | y = k)P(y = k)}{\sum_{l=1}^L P(\mathbf{x} | y = l)P(y = l)}. \quad (6)$$

If the conditional probability  $P(\mathbf{x} | y = k)$  belongs to the same family of distributions for all  $k \in [L]$ , i.e.,  $\mathbf{x} | y = k \sim \phi(\mathbf{x}; \boldsymbol{\theta}_k)$ , then the probability  $P(\mathbf{x} | y = k)P(y = k)$  can be estimated by (i) estimating the parameters  $\boldsymbol{\theta}_k$  and  $P(y = k)$  and (ii) approximating the function  $\phi$ .

However, the distribution family  $\phi(\mathbf{x}; \boldsymbol{\theta}_k)$  may vary greatly across tasks. To alleviate the task dependency, we use the task-dependent transformation block to allow the transformed covariates to be in the same distribution family approximately. We then utilize the task-independent distribution embedding block to estimate the parameters. Finally, we use the task-independent classification block to approximate the function and obtain a score for each label.

Since the input dimension can vary across tasks, we decompose the covariate vector into sub-vectors of fixed length  $r$  and apply a Deep Sets architecture to these sub-vectors. In fact, if we consider the following family of densities, then the Bayes classifier must be of the form (3).

**Definition 4.2.** Let  $\{f(\cdot; \boldsymbol{\theta}) : \mathbb{R}^r \rightarrow \mathbb{R}\}$  be a parametric family of functions (not necessarily densities). For any integer  $d \geq r$ , we say a function  $g$  on  $\mathbb{R}^d$  admits an *f-expansion* if it factorizes as  $g(\mathbf{z}) = \prod_{t_{1:r} \in [d]^r} f(\mathbf{z}^{t_{1:r}}; \boldsymbol{\theta}^{t_{1:r}})$ , where  $\{\boldsymbol{\theta}^{t_{1:r}} \in \mathbb{R}^r\}$  is a set of parameters.

For instance, if  $\mathbf{z}|y=1 \sim \mathcal{N}_d(\boldsymbol{\mu}, \sigma^2 I_d)$ , then the conditional density  $p(\mathbf{z}|y=1)$  is proportional to

$$\prod_{a=1}^d \frac{1}{\sigma} \exp\left(-\frac{(z^a - \mu^a)^2}{2\sigma^2}\right),$$

which admits an *f-expansion* with  $r = 1$  and  $\boldsymbol{\theta}^a = (\mu^a, \sigma)$ .

**Proposition 4.3.** *Let  $(\mathbf{z}, y)$  be a random vector in  $\mathbb{R}^d \times [L]$  following some distribution  $P$ . Assume that the conditional density  $p(\mathbf{z}|y = k)$  admits an  $f$ -expansion for some parametric family of functions  $\{f(\cdot; \boldsymbol{\theta})\}$  on  $\mathbb{R}^r$  with parameters  $\{\boldsymbol{\theta}_k^{t_{1:r}}\}$ . Then there exist functions  $\psi$  and  $\varphi$  such that*

$$P(y = k | \mathbf{z}) \propto \psi \left( \sum_{t_{1:r} \in [d]^r} \varphi(\mathbf{z}^{t_{1:r}}, \boldsymbol{\theta}_k^{t_{1:r}}, \pi_k) \right), \quad (7)$$

where  $\mathbf{z}^{t_{1:r}} = (z^{t_1}, \dots, z^{t_r})$ ,  $\pi_k = P(y = k)$ , and  $\psi$  and  $\varphi$  only depend on  $f$ .

The proof is included in Appendix A. Due to Proposition 4.3, if the conditional density  $p(\mathbf{z}|y = k)$  admits the same  $f$ -expansion for all  $k \in [L]$  across tasks, then the optimal Bayes classifier has the form in (7) with task-independent functions  $\psi$  and  $\varphi$ . This justifies our choice of the distribution embedding in (2) and the Deep Sets structure in (3).

## 4.4 Training and Inference

Figure 2 shows a high level summary of our three-block model architecture. The overall training and evaluation procedure is summarized in Table 1. The computational complexity and resource requirement of DEN are similar to those of Vinyals et al. (2016) and Iwata and Kumagai (2020) given similar model sizes.

During pre-training, in each gradient step, we randomly sample a task  $\mathbb{T} \in \{\mathbb{T}_t\}_{t=1}^M$ , and sample query set  $A$  and support set  $B$  from  $(\mathbf{X}_{\mathbb{T}}, \mathbf{y}_{\mathbb{T}})$ . These two batches of covariates are first transformed using PLFs in (1). We then use (2) or (4) to obtain a distribution embedding  $\mathbf{s}_{\mathbb{T}}$ , taking the average with respect to the examples in the support set  $B$ . Next, we use the distribution embedding to make predictions on query set  $A$  using (3) or (5). Note that during training,  $\mathbf{s}_{\mathbb{T}}$  is identical across examples within the same batch, but it could vary (even within the same task) across batches.

If PLFs can approximately transform the covariates so that they admit the same  $f$ -expansion, then the rest of the network is task-agnostic. Thus, after pre-training on  $\{\mathbb{T}_t\}_{t=1}^M$ , for each new task  $\mathbb{S}$ , we can fine-tune the transformation block (1), while keeping the weights of other blocks fixed. Because PLFs only have a small number of parameters, they can be trained on a small support set from the task  $\mathbb{S}$ .

During inference, we first use the learned PLFs in (1) to transform covariates in both the support set and the query set. We then utilize the learned distribution embedding block to obtain  $\mathbf{s}_{\mathbb{S}}$ , where the average in (2) and (4) is taken over the whole support set. Finally, the embedding  $\mathbf{s}_{\mathbb{S}}$  and PLF-transformed query set covariates are used to classify query set examples using (3) or (5).

## 5 Numerical Studies

In this section, we examine the performance of DEN, as well as the effects of PLF transformation, distribution embedding, and fine-tuning. In Section 5.1, we introduce an approach to simulate tasks, which allows us to generate a huge amount of pre-training examples without the need of collecting real data. In Section 5.2, we use simulated tasks to show that DEN outperforms other methods in aggregating an ensemble of classifiers, and that the effect of PLF and fine-tuning is insignificant when training and test tasks are similar. In Section 5.3, we use two real datasets to show that PLF and fine-tuning are crucial when the training and test tasks are unrelated, and the performance of DEN is relatively stable for small values of the dependency order  $r$  in (2). Since DEN is designed for tabular data we use OpenML tabular datasets to demonstrate the superior performance of DEN on real datasets in Section 5.4. DEN can also be applied to vision data when it is equipped with a pre-trained embedding model, i.e., treat the image embedding as the covariate vector. This is beyond the scope of this paper and we leave it to future work.

Baseline methods for comparison with DEN include Matching Net (Vinyals et al., 2016), Proto Net (Snell et al., 2017), TADAM (Oreshkin et al., 2018), PMN (Wang et al., 2018), Relation Net (Sung et al., 2018), CNP (Garnelo et al., 2018), MAML (Finn et al., 2017), BMAML (Finn et al., 2018), T-Net (Lee and Choi, 2018) and Iwata and Kumagai (2020). Hyperparameters of all methods are chosen based on cross-validation on



training tasks. Hyperparameters, model structures and implementation details are summarized in Appendix B. Note that we set the dependency order  $r = 2$  if it is not stated explicitly. For MAML, BMAML and T-net, we fine-tune the last layer of the base model for 5 epochs on the support set. For the rest of the methods, we train them with episodic training Vinyals et al. (2016).

## 5.1 Generate Training Tasks through Controlled Simulation

We describe an approach to generate binary classification training tasks based on ensemble aggregation. Comparing to pre-training meta-learning models on real datasets, which could be expensive to collect, this synthetic approach can easily give us a huge amount of pre-training examples. We will show in Section 5.4 that meta-learning methods trained with simulated data can sometimes outperform those trained with real data.

Specifically, we first take seven image classification datasets: CIFAR-10, CIFAR-100 (Krizhevsky, 2009), MNIST (LeCun et al., 2010), Fashion MNIST (Xiao et al., 2017), EMNIST (Cohen et al., 2017), Kuzushiji MNIST (KMNIST; Clanuwat et al., 2018) and SVHN (Netzer et al., 2011). On each dataset, we pick nine equally spaced cutoffs and binarize the labels based on whether the class id is below the cutoff. This gives rise to nine binary classification tasks for each dataset with positive label proportion in  $\{0.1, 0.2, \dots, 0.9\}$ . In summary, we collect  $7 \times 9 = 63$  binary classification tasks  $\{\mathbb{T}_1, \dots, \mathbb{T}_{63}\}$ .

To generate covariates for each task, we build 50 convolutional image classifiers of various model complexities (details in Appendix B) on each of the 63 tasks to predict the binary label. We take classification scores on the test set as covariates  $\mathbf{x}_{\mathbb{T}} \in [0, 1]^{50}$ . Note that the accuracy of those image classifiers ranges from below 0.6 to over 0.99, giving rise to covariates ranging widely in their signal-to-noise ratios. The number of training examples in each task is equal to the size of the corresponding test set.

Finally, to augment training data, we apply covariate sampling during training. In each pre-training step, after selecting one of the 63 tasks, we randomly pick  $C < 50$  covariates from the task to construct a *sub-task*, and use it for training in this step. The number  $C$  could vary across training steps, creating a diverse set of covariate spaces.

## 5.2 Meta-Learning on Model Aggregation

We study the performance of DEN in aggregating an ensemble of classifiers. We also study the impact of fine-tuning PLF on the performance of DEN. As discussed in Section 4, fine-tuning PLF is a powerful way to adapt DEN to a wide variety of tasks with different input distributions. However, in the scenario when the distributions of training and target tasks are similar, fine-tuning PLF can introduce overfitting that outweighs its benefit, especially when the support set is small compared to the number of covariates.

We use the  $5 \times 9 = 45$  tasks described in Section 5.1 derived from CIFAR-10, CIFAR-100, MNIST, Fashion MNIST and EMNIST to train DEN and other meta-learning methods. We then pick four test tasks from SVHN and KMNIST of different difficulties, where the average AUC over 50 classifiers is 68.28%, 78.11%, 91.51%, and 87.58%, respectively. For each test task, we randomly select 100 sets of  $C$  classifiers among the 50 candidate classifiers, resulting in 100 aggregation sub-tasks. For each aggregation sub-task, we form a support set with 50 labeled examples and a disjoint query set with 8000 examples. For DEN, we explore three options, 1) fine-tune the PLF layer for 10 epochs, 2) take the PLF layer directly from the last pre-training epoch without fine-tuning, or 3) do not include a PLF layer in DEN and hence no fine-tuning at all. We repeat the entire training and fine-tuning process for 5 times, and report the average AUC and its standard error.

Table 2 shows the result of aggregating an ensemble of  $C = 25$  classifiers. Table 3 shows the result where the number of classifiers  $C$  to be aggregated is sampled uniformly from  $[13, 25]$  and could vary across sub-tasks (100 aggregation sub-tasks  $\times$  5 repeats). To allow baseline methods to take varying number of covariates, we randomly duplicate some of the  $C$  classifiers so that all inputs have 25 covariates.

We observe that DEN significantly outperforms other methods in all tasks. We also observe that DEN without PLF and/or without fine-tuning is statistically no worse than DEN with fine-tuning on the PLF

Table 2: Test % AUC (standard error) when aggregating 25 classifiers.

Method	Test AUC (%)			
	Task 1	Task 2	Task 3	Task 4
Matching Net	70.01 (0.40)	82.13 (0.05)	95.29 (0.06)	93.82 (0.08)
Proto Net	90.95 (0.05)	89.84 (0.03)	98.07 (0.01)	97.40 (0.02)
TADAM	90.98 (0.05)	89.90 (0.03)	98.14 (0.01)	97.57 (0.02)
PMN	86.78 (0.10)	88.69 (0.03)	97.46 (0.02)	96.22 (0.05)
Relation Net	85.39 (0.15)	88.70 (0.02)	97.25 (0.02)	95.55 (0.08)
CNP	86.53 (0.09)	88.80 (0.02)	97.50 (0.02)	96.22 (0.05)
<a href="#">Iwata and Kumagai (2020)</a>	89.33 (0.05)	89.17 (0.02)	97.93 (0.01)	97.73 (0.02)
MAML	86.10 (0.11)	88.78 (0.03)	97.48 (0.02)	96.13 (0.06)
BMAML	71.38 (0.84)	85.96 (0.21)	97.04 (0.08)	95.39 (0.18)
T-Net	86.23 (0.10)	88.76 (0.03)	97.47 (0.02)	96.11 (0.06)
DEN w/o PLF w/o Fine-Tuning	91.53 (0.03)	<b>90.18</b> (0.02)	98.03 (0.01)	98.37 (0.01)
DEN w/o Fine-Tuning	<b>91.76</b> (0.03)	<b>90.20</b> (0.02)	<b>98.18</b> (0.01)	<b>98.41</b> (0.01)
DEN	<b>91.80</b> (0.03)	89.77 (0.02)	97.38 (0.01)	97.23 (0.01)

Table 3: Test % AUC (standard error) when aggregating variable number of classifiers.

Method	Test AUC (%)			
	Task 1	Task 2	Task 3	Task 4
Matching Net	75.16 (0.37)	81.12 (0.08)	95.86 (0.04)	93.61 (0.08)
Proto Net	90.02 (0.11)	89.65 (0.04)	97.94 (0.02)	97.57 (0.02)
TADAM	90.20 (0.10)	89.74 (0.04)	98.04 (0.01)	97.84 (0.01)
PMN	85.68 (0.24)	88.59 (0.04)	97.30 (0.03)	95.83 (0.08)
Relation Net	80.85 (0.65)	88.53 (0.04)	97.11 (0.04)	95.03 (0.12)
CNP	84.97 (0.28)	88.71 (0.04)	97.31 (0.04)	95.96 (0.07)
<a href="#">Iwata and Kumagai (2020)</a>	89.26 (0.16)	89.05 (0.03)	97.82 (0.02)	97.75 (0.02)
MAML	85.39 (0.23)	88.53 (0.04)	97.32 (0.04)	95.86 (0.08)
BMAML	59.57 (1.07)	85.40 (0.24)	96.73 (0.10)	94.53 (0.23)
T-Net	85.51 (0.22)	88.55 (0.04)	97.35 (0.03)	95.94 (0.07)
DEN w/o PLF w/o Fine-Tuning	91.06 (0.09)	<b>89.92</b> (0.03)	<b>98.09</b> (0.01)	<b>98.24</b> (0.01)
DEN w/o Fine-Tuning	<b>91.17</b> (0.09)	<b>89.95</b> (0.03)	97.95 (0.01)	98.10 (0.01)
DEN	<b>91.29</b> (0.03)	89.83 (0.02)	97.60 (0.03)	97.47 (0.01)

layer. This suggests that fine-tuning the PLF layer is not necessary when the input distribution is similar among training and test tasks.

### 5.3 Effect of Dependence Order, PLF, and Fine-tuning

We study and demonstrate the importance of PLF when the training and test tasks have heterogeneous covariate distributions. Specifically, we use all 63 tasks described in the first subsection in pre-training, and test the performance on two real datasets: Nomao and Puzzles. We give a short description of each dataset below, and list the covariates in Appendix C.



Table 4: Test % AUC (standard error) on Nomao and Puzzles data.

Method	Nomao	Puzzles
Matching Net	73.18 (2.23)	62.65 (1.45)
Proto Net	80.56 (0.56)	73.77 (0.37)
TADAM	82.42 (0.35)	74.86 (0.25)
PMN	77.00 (3.13)	57.69 (1.53)
Relation Net	52.32 (1.61)	63.73 (1.79)
CNP	91.40 (0.36)	53.20 (0.12)
Iwata and Kumagai (2020)	66.85 (3.23)	61.32 (0.52)
MAML	78.92 (2.22)	54.92 (0.54)
BMAML	47.20 (3.40)	53.49 (1.88)
T-Net	61.42 (3.44)	54.55 (1.78)
DEN w/o PLF w/o FT	59.01 (1.04)	68.87 (0.38)
DEN w/o FT	94.42 (0.16)	70.74 (0.62)
DEN	<b>95.21</b> (0.10)	<b>78.11</b> (0.53)

- With Nomao data<sup>2</sup>, we use seven covariates to classify whether two entities are identical. There are 50 examples in the support set.
- With Puzzles data<sup>3</sup>, we use six covariates to classify whether the number of units sold for each puzzle in a six months period is above 45. The support set (with 155 puzzles) covers the first six months period, whereas the non-iid query set (with 367 puzzles) covers the second and third six months periods.

For each dataset, we repeat the whole procedure 20 times and report the average AUC and standard error in Table 4. It is clear that DEN outperforms other baseline methods significantly. More importantly, the results also show that fine-tuning and PLF greatly improve the performance of DEN, demonstrating their importance when the pre-training and target tasks have heterogeneous distributions.

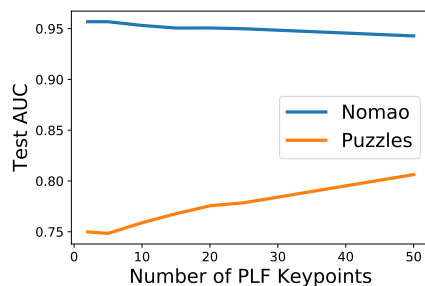


Figure 3: Test AUC versus the number of PLF keypoints.

We also examine the effect of the size of the support set on the flexibility of the covariate transformation block. Figure 3 shows that with enough support set examples (e.g., Puzzles task), having more PLF keypoints benefits the test performance due to the improved ability of task-adaptation. However, if the support set is small (e.g., Nomao task), having a flexible covariate transformation block may not be helpful, and could even be marginally harmful.

<sup>2</sup><https://archive.ics.uci.edu/ml/datasets/Nomao>

<sup>3</sup><https://www.kaggle.com/dbahri/puzzles>

Table 5: Test % AUC (standard error) of DEN on Nomao data with different dependency order .

$r = 1$	$r = 2$	$r = 3$	$r = 4$
94.38 (0.46)	<b>95.21</b> (0.10)	93.80 (0.25)	92.61 (0.55)
$r = 5$	$r = 6$	$r = 7$	$r = 8$
93.16 (0.45)	91.22 (0.74)	88.95 (2.02)	89.15 (1.34)

Table 6: Test % AUC (standard error) and the percent of times that each method achieves the best performance on 20 OpenML datasets  $\times$  20 repeats. We consider pre-training on either simulated data or OpenML datasets.

Method	Pre-train on Simulated Data		Pre-train on OpenML Data	
	Average Test AUC (%)	% Best	Average Test AUC (%)	% Best
Matching Net	53.88 (0.46)	0.00%	50.11 (0.04)	0.00%
Proto Net	71.12 (0.65)	28.00%	<b>71.11</b> (0.72)	27.50%
PMN	59.04 (0.68)	1.25%	56.11 (0.65)	0.75%
Relation Net	57.97 (0.59)	0.00%	51.65 (0.28)	0.25%
CNP	60.95 (0.69)	2.50%	58.01 (0.69)	7.00%
<a href="#">Iwata and Kumagai (2020)</a>	66.01 (0.74)	11.50%	<b>70.35</b> (0.70)	26.75%
MAML	61.16 (0.66)	2.75%	60.64 (0.82)	7.00%
T-Net	53.35 (0.46)	0.25%	52.22 (0.41)	0.5%
DEN	<b>74.13</b> (0.68)	<b>53.75%</b>	<b>70.12</b> (0.83)	<b>30.25%</b>

Finally, we conduct an ablation study to examine the effect of dependency order in (2) on the test AUC on the Nomao dataset. In particular, we examine DEN with  $r \in [8]$ . The results in Table 5 show that when  $r \leq 5$ , the test AUC is relatively stable, with the best performance achieved when  $r = 2$ ; whereas the test AUC is much worse and unstable for larger  $r$ .

## 5.4 Meta-Learning on OpenML Classification Tasks

**Binary classification.** We compare DEN with baseline methods on 20 OpenML binary classification datasets [Vanschoren et al. \(2013\)](#) following the setup in [Iwata and Kumagai \(2020\)](#) (see a list of datasets in Appendix C). These datasets have examples ranging from 200 to 1,000,000 and features ranging from 2 to 25.

We pre-train DEN and baseline methods on the OpenML datasets in the leave-one-dataset-out fashion. That is, for each of the 20 OpenML datasets chosen as a target task, we pre-train the models on the remaining 19 datasets. For the target task, we randomly select 50 examples to form the support set, and use the rest of the dataset as the test set. We repeat the whole procedure 20 times, and report the average AUC and the percentage of times each method achieves the best performance in Table 6 based on 20 test sets  $\times$  20 repeats. DEN has average AUC comparable with the best method, and the frequency that it achieves the best AUC is highest among all methods.

To illustrate the effectiveness of data simulation approach described in Section 5.1, we use the models pre-trained on these data and evaluate them on 20 OpenML datasets after fine-tuning. Interestingly, all of the models but [Iwata and Kumagai \(2020\)](#) achieve better average AUC if they are pre-trained on the simulated data. This suggests that the proposed approach to generate training tasks is not only convenient but also effective. Moreover, DEN pre-trained on the simulated data outperforms all methods (either pre-trained on the simulated data or OpenML data) significantly.

Table 7: Test multiclass accuracy (standard error) and the percent of times that each method achieves the best performance on 8 OpenML datasets  $\times$  20 repeats.

Method	Accuracy (%)	% Best
Direct DNN	<b>45.68</b> (1.56)	13.6%
Matching Net	<b>46.36</b> (1.55)	13.8%
Proto Net	33.68 (1.80)	4.9%
PMN	24.77 (0.63)	0.0%
Relation Net	33.49 (1.82)	4.9%
CNP	18.77 (1.53)	1.1%
<a href="#">Iwata and Kumagai (2020)</a>	24.93 (0.62)	0.0%
DEN	<b>48.60</b> (1.51)	<b>61.6%</b>

**Multiclass classification.** Finally, we compare DEN with baseline methods on 8 OpenML multi-class classification datasets. These datasets have examples ranging from 400 to 1,000,000, features ranging from 5 to 23, and number of classes ranging from 3 to 7. We train DEN and baseline methods on the OpenML datasets in the same leave-one-dataset-out fashion as in the binary classification. Results are summarized in Table 7. DEN achieved the best performance, followed by Matching Net. We also compare against directly training a DNN model on the support set, which achieves decent accuracy. But DEN remains the best methods in majority (61.6%) of cases.

## 6 Conclusion

In this paper, we introduce a novel meta-learning method that can be applied to settings where both the distribution and number of covariates vary across tasks. This allows us to train the model on a wider range of training tasks and then adapt it to a variety of test tasks. Most other meta-learning techniques do not readily handle such settings. In numerical studies, we demonstrate that the proposed method outperforms a number of meta-learning baselines.

The proposed model consists of three flexible building blocks. Each block can be replaced by more advanced structures to further improve its performance. For instance, for the covariate transformation block, we may use pairwise transformations instead of one-dimensional PLFs to account for associations between covariates; for the classification block, based on results from earlier work, using a Set Transformer structure instead of a Deep Sets one may give us improved performance. DEN can also be combined with optimization based meta-learning methods, e.g., MAML. A current limitation of DEN is that it requires calculating the embedding for  $d^r$  different combinations of covariates, which is infeasible for high-dimensional tasks. A potential solution is to use a random subset of these combinations. We leave the exploration of these options to future work.

## References

- L. Bertinetto, J. F. Henriques, J. Valmadre, P. H. S. Torr, and A. Vedaldi. Learning feed-forward one-shot learners. In *NIPS*, 2016.
- T. Clanuwat, M. Bober-Irizar, A. Kitamoto, A. Lamb, K. Yamamoto, and D. Ha. Deep learning for classical Japanese literature. *NeurIPS Workshop on Machine Learning for Creativity and Design*, 2018.
- G. Cohen, S. Afshar, J. Tapson, and A. V. Schaik. EMNIST: Extending MNIST to handwritten letters. In *IJCNN*, 2017.

- W. Dai, Y. Chen, G. Xue, Q. Yang, and Y. Yu. Translated learning: Transfer learning across different feature spaces. In *NIPS*, 2008.
- O. Day and T. M. Khoshgoftaar. A survey on heterogeneous transfer learning. *Journal of Big Data*, 4, 2017.
- L. Duan, D. Xu, and I. W. Tsang. Learning with augmented features for heterogeneous domain adaptation. In *ICML*, 2012.
- H. Edwards and A. Storkey. Towards a neural statistician. In *ICLR*, 2017.
- C. Finn, P. Abbeel, and S. Levine. Model-agnostic meta-learning for fast adaptation of deep networks. In *ICML*, 2017.
- C. Finn, K. Xu, and S. Levine. Probabilistic model-agnostic meta-learning. In *NeurIPS*, 2018.
- M. Garnelo, D. Rosenbaum, C. Maddison, T. Ramalho, D. Saxton, M. Shanahan, Y. W. Teh, D. Rezende, and S. M. A. Eslami. Conditional neural processes. In *ICML*, 2018.
- E. Grant, C. Finn, S. Levine, T. Darrell, and T. Griffiths. Recasting gradient-based meta-learning as hierarchical Bayes. In *ICLR*, 2018.
- M. Gupta, A. Cotter, J. Pfeifer, K. Voevodski, K. Canini, A. Mangylov, W. Moczydlowski, and A. van Esbroeck. Monotonic calibrated interpolated look-up tables. *Journal of Machine Learning Research*, 17 (109), 2016.
- T. Iwata and A. Kumagai. Meta-learning from tasks with heterogeneous attribute spaces. In *NeurIPS*, 2020.
- L. Kaiser, O. Nachum, A. Roy, and S. Bengio. Learning to remember rare events. In *ICLR*, 2017.
- G. Koch, R. Zemel, and R. Salakhutdinov. Siamese neural networks for one-shot image recognition. In *ICML*, 2015.
- A. Krizhevsky. Learning multiple layers of features from tiny images. Technical report, University of Toronto, 2009.
- Y. LeCun, C. Cortes, and C. Burges. MNIST handwritten digit database. *ATT Labs [Online]*. Available: <http://yann.lecun.com/exdb/mnist>, 2010.
- J. Lee, Y. Lee, J. Kim, A. Kosiorek, S. Choi, and Y. W. Teh. Set Transformer: A framework for attention-based permutation-invariant neural networks. In *ICML*, 2019.
- Y. Lee and S. Choi. Gradient-based meta-learning with learned layerwise metric and subspace. In *ICML*, 2018.
- W. Li, L. Duan, D. Xu, and I. W. Tsang. Learning with augmented features for supervised and semi-supervised heterogeneous domain adaptation. *IEEE Transactions on Pattern Analysis and Machine Intelligence*, 36 (6), 2014.
- Y. Liu, J. Lee, M. Park, S. Kim, E. Yang, S. Hwang, and Y. Yang. Learning to propagate labels: Transductive propagation network for few-shot learning. In *ICLR*, 2019.
- N. Mishra, M. Rohaninejad, X. Chen, and P. Abbeel. A simple neural attentive meta-learner. In *ICLR*, 2018.
- T. Munkhdalai and H. Yu. Meta networks. In *ICML*, 2017.
- T. Munkhdalai, X. Yuan, S. Mehri, and A. Trischler. Rapid adaptation with conditionally shifted neurons. In *ICML*, 2018.

- Y. Netzer, T. Wang, A. Coates, A. Bissacco, B. Wu, and A. Y. Ng. Reading digits in natural images with unsupervised feature learning. *NIPS Workshop on Deep Learning and Unsupervised Feature Learning*, 2011.
- B. N. Oreshkin, P. R. López, and A. Lacoste. TADAM: task dependent adaptive metric for improved few-shot learning. In *NeurIPS*, 2018.
- S. Ravi and H. Larochelle. Optimization as a model for few-shot learning. In *ICLR*, 2017.
- A. A. Rusu, D. Rao, J. Sygnowski, O. Vinyals, R. Pascanu, S. Osindero, and R. Hadsell. Meta-learning with latent embedding optimization. In *ICLR*, 2019.
- A. Santoro, S. Bartunov, M. Botvinick, D. Wierstra, and T. Lillicrap. Meta-learning with memory-augmented neural networks. In *ICML*, 2016.
- V. G. Satorras and J. B. Estrach. Few-shot learning with graph neural networks. In *ICLR*, 2018.
- J. Snell, K. Swersky, and R. S. Zemel. Prototypical networks for few-shot learning. In *NIPS*, 2017.
- F. Sung, Y. Yang, L. Zhang, T. Xiang, P. H. S. Torr, and T. M. Hospedales. Learning to compare: Relation network for few-shot learning. In *CVPR*, 2018.
- J. Vanschoren, J. N. van Rijn, B. Bischl, and L. Torgo. Openml: Networked science in machine learning. *SIGKDD Explorations*, 15(2), 2013.
- O. Vinyals, C. Blundell, T. Lillicrap, K. Kavukcuoglu, and D. Wierstra. Matching networks for one shot learning. In *NIPS*, 2016.
- C. Wang and S. Mahadevan. Heterogeneous domain adaptation using manifold alignment. In *IJCAI*, 2011.
- Y. Wang, R. Girshick, M. Hebert, and B. Hariharan. Low-shot learning from imaginary data. In *CVPR*, 2018.
- Y. Wang, Q. Yao, J. T. Kwok, and L. M. Ni. Generalizing from a few examples: A survey on few-shot learning. *ACM Computing Surveys*, 53(3), 2020.
- H. Xiao, K. Rasul, and R. Vollgraf. Fashion-MNIST: a novel image dataset for benchmarking machine learning algorithms. *ArXiv preprint*, 2017.
- Y. Yan, W. Li, M. K. P. Ng, M. Tan, H. Wu, H. Min, and Q. Wu. Learning discriminative correlation subspace for heterogeneous domain adaptation. In *IJCAI*, 2017.
- Q. Yang, Y. Chen, G.-R. Xue, W. Dai, and Y. Yu. Heterogeneous transfer learning for image clustering via the social web. In *Proceedings of the 47th Annual Meeting of the ACL and the 4th IJCNLP of the AFNLP*, 2009.
- M. Zaheer, S. Kottur, S. Ravanbakhsh, B. Póczos, R. Salakhutdinov, and A. J. Smola. Deep sets. In *NIPS*, 2017.
- J. T. Zhou, S. J. Pan, I. W. Tsang, and Y. Yan. Hybrid heterogeneous transfer learning through deep learning. In *AAAI*, 2014.
- J. T. Zhou, I. W. Tsang, S. J. Pan, and M. Tan. Multi-class heterogeneous domain adaptation. *Journal of Machine Learning Research*, 20, 2019.

## A Details and Proofs

**Piecewise linear function.** The piecewise linear function (PLF)  $c_{\mathbb{T}}^j : \mathbb{R} \rightarrow \mathbb{R}$  for each covariate  $j$  and task  $\mathbb{T}$  is defined by

$$c_{\mathbb{T}}^j(x; \mathbf{k}_{\mathbb{T}}^j, \boldsymbol{\alpha}_{\mathbb{T}}^j) := \sum_{l=1}^{K-1} \mathbb{1} \left( k_{\mathbb{T},l}^j \leq x \leq k_{\mathbb{T},l+1}^j \right) \ell_{\mathbb{T},l}^j(x), \quad (8)$$

$$\ell_{\mathbb{T},l}^j(x) := \alpha_{\mathbb{T},l}^j + \frac{x - k_{\mathbb{T},l}^j}{k_{\mathbb{T},l+1}^j - k_{\mathbb{T},l}^j} \left( \alpha_{\mathbb{T},l+1}^j - \alpha_{\mathbb{T},l}^j \right),$$

where  $\mathbf{k}_{\mathbb{T}}^j := [k_{\mathbb{T},1}^j, \dots, k_{\mathbb{T},K}^j] \in \mathbb{R}^K$ ,  $k_{\mathbb{T},1}^j < k_{\mathbb{T},2}^j < \dots < k_{\mathbb{T},K}^j$ , is the vector of *predetermined* keypoints that spans the domain of  $x_{\mathbb{T}}^j$ , and  $\boldsymbol{\alpha}_{\mathbb{T}}^j := [\alpha_{\mathbb{T},1}^j, \dots, \alpha_{\mathbb{T},K}^j] \in \mathbb{R}^K$  is the parameter vector, characterizing the output at each keypoint.

*Proof of Proposition 4.3.* By the Bayes' rule, for each  $k \in [L]$ ,

$$P(y = k | \mathbf{z}) \propto p(\mathbf{z} | y = k) p(y = k) = \pi_k \prod_{t_{1:r} \in [d]^r} f(\mathbf{z}^{t_{1:r}}; \boldsymbol{\theta}_k^{t_{1:r}}).$$

Define the function  $\varphi$  by

$$\varphi(\mathbf{z}^{t_{1:r}}, \boldsymbol{\theta}_k^{t_{1:r}}, \pi_k) = \log f(\mathbf{z}^{t_{1:r}}; \boldsymbol{\theta}_k^{t_{1:r}}) + \frac{1}{d^r} \log \pi_k,$$

and define  $\psi(x) = e^x$ . Then it is clear that

$$P(y = k | \mathbf{z}) \propto \psi \left( \sum_{t_{1:r} \in [d]^r} \varphi(\mathbf{z}^{t_{1:r}}, \boldsymbol{\theta}_k^{t_{1:r}}, \pi_k) \right).$$

□

## B Model Structures and Hyperparameters

In this section, we report model structures and hyperparameters of all models we have considered in our experiments.

To generate training tasks, the 50 convolutional image classifiers all have the structure  $\text{Conv}(f, k) \rightarrow \text{MaxPool}(p) \rightarrow \text{Conv}(f, k) \rightarrow \text{MaxPool}(p) \rightarrow \dots \rightarrow \text{Conv}(f, k) \rightarrow \text{Dense}(u) \rightarrow \text{Dense}(u) \rightarrow \dots \rightarrow \text{Dense}(1)$ , where the number of dense layers  $d \in [1, 4]$ , number of convoluted layers  $c \in [0, 3]$ , filters and units  $f, u \in [2, 511]$ , kernel and pool sizes  $k, p \in [2, 5]$ , and training epochs  $e \in [1, 24]$  are uniformly sampled.

We use 5-fold cross-validation on  $5 \times 9$  tasks of aggregating 25 classifiers derived from CIFAR-10, CIFAR-100, MNIST, Fashion MNIST and EMNIST to tune the hyperparameters. Note that those 45 tasks were treated as training tasks in all experiments presented in Section 5. In each fold, we trained the model on all but one training datasets and evaluated it on the remaining one<sup>4</sup>, feeding with 50 supporting examples; we then selected the model with the highest AUC scores averaged over 5 folds.

For DEN, Matching Net, Proto Net, TADAM, PMN, Relation Net and CNP, we trained each of them for 200 epochs using Adam optimizer with batch size 256 and the TensorFlow default learning rate, 0.001. We did not apply fine-tuning on those methods.

For MAML, BMAML, T-Net, we first train a base model (either a DNN or a T-Net) for 1000 steps. In each step, we randomly sample 10 sub-tasks of batch size 256 from 36 training tasks. After these 1000 steps,

<sup>4</sup>For example, in one of the five folds, we trained the models on  $4 \times 9$  tasks derived from CIFAR-10, CIFAR-100, MNIST and Fashion MNIST datasets, and evaluated the model on the 9 tasks derived from the EMNIST dataset

we fine-tuned the last layer of the trained DNN or T-net on a support set of size 50 of each validation task for 6 epochs, then evaluated it on the remaining examples of this validation task.

Note that, during hyperparameter tuning, the maximum number of ReLU-activated dense layers we have tried is 12 and the maximum number of units we have tried is 128 for all models. The proposed Joint DEN and Conditional DEN tend to prefer larger models than the rest ones. Based on cross-validation, we arrived at the following model architectures.

**Matching Net.** For Matching Net, we used the formulation with the attention kernel. The full context embedding is examined with the PMN model. Both the  $f$  and  $g$  embedding functions were 1-hidden-layer, 64-unit DNNs with ReLU activation, which output 64-dimensional embeddings.

**Proto Net.** For Proto Net, the embedding model  $f_\phi$  was a 1-hidden-layer, 32-unit DNN with ReLU activation, which outputs 32-dimensional embeddings. The distance metric is taken as the Euclidean norm.

**TADAM.** For TADAM, the task representation model  $f_\phi$  was a 1-hidden-layer, 32-unit DNN with ReLU activation, which outputs 32-dimensional embeddings. The  $\gamma$  and  $\beta$  models were each a 1-hidden-layer, 32-unit DNN with ReLU activation, which each outputs 64 values. The post multipliers  $\gamma_0$  and  $\beta_0$  were ridge regularized with weight 0.01. We modified the weights of the task representation model based on  $\gamma$  and  $\beta$  as in the FILM conditioning layer to get the class representation model. The similarity metric was taken as the Euclidean norm with metric scaling.

**PMN.** For PMN, the embedding model was a 3-hidden-layer, 32-unit ReLU activated DNN with 32-dimensional output. The bidirectional LSTM and attention LSTM each has units. To build the attention LSTM, we use  $K = 8$  ‘‘Process’’ blocks. The distance metric was Euclidean norm.

**Relation Net.** For Relation Net, the  $f_\psi$  embedding model was a 1-hidden-layer, 32-unit DNN with ReLU activation and 32-dimensional output. The relation model  $g_\phi$  was a 2-hidden-layer, 16-unit DNN with ReLU activation.

**CNP.** For CNP, the embedding model  $h_\theta$  was a 1-hidden-layer, 64-unit DNN with ReLU activation and 64 dimensional output. The commutative operation was taken to be average operation. The prediction model  $g_\theta$  was a 2-hidden-layer, 8-unit DNN with ReLU activation.

**MAML.** For MAML, the base model is a 4-hidden-layer, 64 unit ReLU activated DNN model. The MAML learning rates are  $\alpha = 0.01$  for the inner loop and  $\beta = 0.005$  for the outer loop.

**BMAML.** For BMAML, the base model is a 4-hidden-layer, 64 unit ReLU activated DNN model. The BMAML inner loop learning rate is  $\alpha = 0.01$ . The step size parameters  $\gamma_p$  and  $\gamma_q$  were initialized as a constant vector with value 0.00005, and the variance parameters  $v_q$  and  $\sigma_\theta^2$  were initialized as diagonal matrices with value 0.0001.

**T-Net.** For T-Net, the base model is a T-Net with 4 32-unit  $W$  layers and 4 32-unit  $T$  layers (the last, i.e., output,  $T$  layer has 1-unit). The activation function  $\sigma$  is ReLU. The learning rates were  $\alpha = \beta = 0.01$ .

**DEN.** For DEN, we used PLFs with 10 calibration keypoints, uniformly distributed in the input domain. The distribution embedding model was a 3-hidden-layer, 16-unit ReLU activated DNN with 16 dimensional output. We took the mean embedding over the batch to get the distribution embedding. The Deep Sets classification model is a 3-hidden-layer, 64-unit ReLU activated DNN, followed by mean pooling and another 4-hidden-layer, 64-unit ReLU activated DNN.



Data Name	URL	# Fine-Tune Examples	# Test Examples	# Features
BNG Australian	<a href="https://www.openml.org/d/1205">https://www.openml.org/d/1205</a>	50	999950	14
BNG breast-w	<a href="https://www.openml.org/d/251">https://www.openml.org/d/251</a>	50	39316	9
BNG credit-g	<a href="https://www.openml.org/d/40514">https://www.openml.org/d/40514</a>	50	999950	20
BNG heart-statlog	<a href="https://www.openml.org/d/251">https://www.openml.org/d/251</a>	50	999950	13
Hyperplane 10 1E-3	<a href="https://www.openml.org/d/152">https://www.openml.org/d/152</a>	50	999950	10
SEA 50	<a href="https://www.openml.org/d/161">https://www.openml.org/d/161</a>	50	999950	3
ada prior	<a href="https://www.openml.org/d/1037">https://www.openml.org/d/1037</a>	50	4512	14
adult	<a href="https://www.openml.org/d/1590">https://www.openml.org/d/1590</a>	50	48792	14
churn	<a href="https://www.openml.org/d/40701">https://www.openml.org/d/40701</a>	50	4950	20
cleve	<a href="https://www.openml.org/d/40710">https://www.openml.org/d/40710</a>	50	253	13
cpu act	<a href="https://www.openml.org/d/761">https://www.openml.org/d/761</a>	50	8142	21
default-of-credit-card-clients	<a href="https://www.openml.org/d/42477">https://www.openml.org/d/42477</a>	50	29950	23
disclosure x tampered	<a href="https://www.openml.org/d/795">https://www.openml.org/d/795</a>	50	612	3
fri c2 250 25	<a href="https://www.openml.org/d/794">https://www.openml.org/d/794</a>	50	200	25
fri c3 250 10	<a href="https://www.openml.org/d/793">https://www.openml.org/d/793</a>	50	200	10
irish	<a href="https://www.openml.org/d/451">https://www.openml.org/d/451</a>	50	450	5
phoneme	<a href="https://www.openml.org/d/1489">https://www.openml.org/d/1489</a>	50	5354	5
strikes	<a href="https://www.openml.org/d/770">https://www.openml.org/d/770</a>	50	575	6
sylvine	<a href="https://www.openml.org/d/41146">https://www.openml.org/d/41146</a>	50	5074	20
wholesale-customers	<a href="https://www.openml.org/d/41146">https://www.openml.org/d/41146</a>	50	390	8

Table 8: List of statistics of 20 OpenML binary classification datasets used in numerical studies.

Data Name	URL	# Fine-Tune Examples	# Test Examples	# Features	# Classes
BNG Glass	<a href="https://www.openml.org/d/265">https://www.openml.org/d/265</a>	50	137731	10	7
BNG Vehicle	<a href="https://www.openml.org/d/268">https://www.openml.org/d/268</a>	50	999950	19	4
BNG Page-Blocks	<a href="https://www.openml.org/d/259">https://www.openml.org/d/259</a>	50	295195	11	5
Cars1	<a href="https://www.openml.org/d/40700">https://www.openml.org/d/40700</a>	50	342	8	3
CPMP 2015	<a href="https://www.openml.org/d/41919">https://www.openml.org/d/41919</a>	50	477	23	4
AutoUniv	<a href="https://www.openml.org/d/1553">https://www.openml.org/d/1553</a>	50	650	13	3
Vertebra Column	<a href="https://www.openml.org/d/1523">https://www.openml.org/d/1523</a>	50	260	7	3
Wall Robot Navigation	<a href="https://www.openml.org/d/1526">https://www.openml.org/d/1526</a>	50	5406	5	4

Table 9: List of statistics of 8 OpenML multiclass classification datasets used in numerical studies.

## C Description of Real Datasets

With Nomao data, we use fax trigram similarity score, street number trigram similarity score, phone trigram similarity score, clean name trigram similarity score, geocoder input address trigram similarity score, coordinates longitude trigram similarity score and coordinates latitude trigram similarity score to classify whether two businesses are identical. Positive examples account for 71% of the data. All of the covariates are outputs from some other models, and are expected to be monotonic. Six and seven of the covariates have missing values. Fax trigram similarity score is missing 97% of the time; phone trigram similarity score is missing 58% of the time; street number trigram similarity score is missing 35% of the time; geocoder input address trigram similarity score is missing 0.1% of the time, and both coordinates longitude trigram similarity score and coordinates latitude trigram similarity score are missing 55% of the time.

With Puzzles data, we use has photo (whether the reviews has a photo), is amazon (whether the reviews were on Amazon), number of times users found the reviews to be helpful, total number of reviews, age of the reviews and number of words in the reviews to classify whether the units sold for the respective puzzle is above 45. The cutoff results in positive label proportions of 49% in the support set, and 51% in the query set. Most of the covariates have unknown monotonicity in their effect in the label.

The 20 OpenML binary classification datasets we used in the numerical studies are listed in Table 8. The 8 multiclass classification datasets are listed in Table 9.

## D Description of Numerical Studies

Numerical studies are done with TensorFlow 2 library, ran on the Ubuntu operating system. All training are done on CPU, with 128 GB memory. PLF functions are implemented in the TensorFlow Lattice 1.0 library. In numerical studies, we fixed the random seed to be 91620. Code of numerical studies will be open-sourced upon the acceptance of this paper.

In the ablation study of the dependency order  $r$ , we used the same DEN architecture as described in Appendix B. For cases with  $r \neq 0$ , to avoid exponential growth of the number of r-index sets in the classification block, we randomly selected  $[d]^2$  r-index sets to be used in the classification network (3).